

$^{90}\text{Zr}(p,p')$ Reaction at 18.8 MeV and the Nuclear-Shell Model*W. S. GRAY,[†] R. A. KENEVICK,[‡] AND J. J. KRAUSHAAR*Department of Physics and Astrophysics, University of Colorado, Boulder, Colorado*

AND

G. R. SATCHLER

Oak Ridge National Laboratory, Oak Ridge, Tennessee

(Received 29 September 1965)

The elastic and inelastic scattering of 18.8-MeV protons from ^{90}Zr has been studied. Angular distributions for the elastic and 17 inelastic groups were measured. An optical-model analysis of the elastic scattering was performed. The inelastic scattering was compared with the predictions of the shell model using a simple two-body interaction between the incident and target nucleons. A Yukawa potential with a range of about 1 F and a strength of about 200 MeV gives a good fit to the excitation of the states of the $g_{9/2}$ configuration. Excitation of the other states is discussed in terms of the shell-model configurations expected to contribute. Arguments are given for the spin-flip strength being small.

I. INTRODUCTION

IN recent years a large amount of data on the inelastic scattering of protons has been analyzed in terms of the collective model of the nucleus. It was natural to use this model for those states which were excited strongly and which, in some sense, could be regarded as collective. The experimental data available have ensured that most intensive study has been made of those states which are thought of as quadrupole (2^+) or octupole (3^-) vibrations. However, there are many nuclei for which it would seem more appropriate to use the shell-model description, and it is of interest to study inelastic scattering from these nuclei in terms of this model. This can be done by taking the interaction as a sum of two-body interactions between the projectile and each target nucleon.¹ This will almost certainly be an "effective" interaction, hence to obtain information about it we require experimental data for transitions between states whose wave functions we believe we know reasonably well. The nucleus ^{90}Zr is a promising subject for study since it possesses a set of excited states which are well described by the shell model in terms of relatively pure ($p_{1/2}g_{9/2}$) and ($g_{9/2}$)² configurations,² as well as a highly collective low-lying 3^- octupole state.³ Therefore, the angular distributions and absolute cross sections for these states can form a

test for the theory and determine values for interaction parameters not coming directly out of the theory. ^{90}Zr is also attractive from the experimental point of view for several reasons. First, isotopically enriched thin metallic foil is available. Secondly, the general level spacing, except for the near degeneracy of the 3^- and 4^- states at 2.75 MeV, is sufficiently large to permit the use of solid-state detectors, with a characteristic energy resolution of 50–100 keV.

This order of energy resolution is also well within the capabilities of the University of Colorado variable energy AVF cyclotron.⁴ Finally, the thickness of solid-state detector required (about 2 mm) for 18.8-MeV protons allowed the use of reliable surface-barrier types.⁵

II. EXPERIMENTAL METHOD

The ^{90}Zr target material was obtained from the Separated Isotopes Division of the Oak Ridge National Laboratory in the form of a metallic foil 2.39 ± 0.05 mg/cm² thick and enriched to 97.8% ^{90}Zr . The thickness was determined in two ways: by direct weighing and by measuring the energy loss for 5.477-MeV α particles emitted by a thin ^{241}Am source. The thickness from these methods agreed within the above-stated error.

Data were obtained in the 91.5-cm scattering chamber facility at the University of Colorado Nuclear Physics Laboratory. Remote controlled arms and drives within this chamber allowed determination of target and detector angle to within $\pm 1^\circ$. The 2-mm surface-barrier solid-state detector⁶ was located on a movable arm 20 cm from the target. The solid angle was determined by a single 4.75-mm diameter circular aperture directly in front of the detector. The silicon detector was shielded from neutrons, β rays, and γ rays by a 1.27-cm-thick copper housing. In order to obtain the best resolution

* Research sponsored by the U. S. Atomic Energy Commission under contracts with the Union Carbide Corporation, and with the University of Colorado.

[†] Present address: University of Michigan, Ann Arbor, Michigan.

[‡] Present address: Texas A & M University, College Station, Texas.

¹ This model has been used by a number of authors; for example, C. A. Levinson and M. K. Banerjee, *Ann. Phys. (N.Y.)* **2**, 471 (1957); N. K. Glendenning, *Phys. Rev.* **114**, 1297 (1959); W. T. Pinkston and G. R. Satchler, *Nucl. Phys.* **27**, 270 (1960); H. O. Funsten, N. R. Roberson, and E. Rost, *Phys. Rev.* **134**, B117 (1964).

² B. F. Bayman, A. S. Reiner, and R. K. Sheline, *Phys. Rev.* **115**, 1627 (1959); I. Talmi and I. Unna, *Nucl. Phys.* **19**, 225 (1960).

³ M. Crut, D. R. Sweetman, and N. S. Wall, *Nucl. Phys.* **17**, 655 (1960); R. K. Jolly, E. K. Lin, and B. L. Cohen, *Phys. Rev.* **128**, 2292 (1962); H. W. Broek and J. L. Yntema, *ibid.* **138**, B334 (1965).

⁴ D. A. Lind, J. J. Kraushaar, W. R. Smythe, and M. E. Rickey, *Nucl. Instr. Methods*, **18–19**, 62 (1962).

⁵ For a general discussion of solid-state detectors, see *IRE Trans. Nucl. Sci.* **NS-7**, No. 2–3 (1960).

⁶ This detector was obtained from the Oak Ridge Technical Enterprises Corporation (ORTEC).

and charge-detection efficiency, a cold trap containing solid CO_2 was placed behind the detector and in thermal contact with it. A flexible tube passed the CO_2 vapors out of the chamber. Operation of the detector at -85°C allowed a higher bias voltage to be applied while keeping the back current at essentially zero. The external proton beam from the cyclotron was focused by a quadrupole magnet, bent 30° in a beam switching magnet and directed onto a two-aperture collimation system mounted in the scattering chamber. The first aperture was 4.75 mm in diameter and the second was slightly larger, in order to stop only beam scattered from the first. The energy spread on the target through this system was typically 40–50 keV and beam intensity up to $0.2\ \mu\text{A}$ was available.

Pulses from the detector were amplified and shaped by an ORTEC Model 101-201 preamplifier-amplifier system and fed directly into a Nuclear Data ND-160 4096-channel pulse-height analyzer (operated in the 4×1024 mode). Integrated beam current and a dead-time correction were obtained automatically by coupling the Faraday cup to a voltage-to-frequency converter whose output was fed into the clock channel of the analyzer.⁷ The dead time was always held to less than 5%, by reducing beam intensity if necessary, and

integrated charge per angular point was varied from $8\ \mu\text{C}$ to $163\ \mu\text{C}$ depending on the importance of the point.

No particle-identification system was found to be necessary in this experiment. The thresholds for (p,d) and (p,t) reactions lie at more than 9-MeV excitation with respect to ^{90}Zr and results of a separate experiment showed that the cross sections for $(p,^3\text{He})$ and (p,α) reactions were negligibly small. In any case the kinematic shift with angle of particles from the latter reactions would show clearly their nature (also, the target was sufficiently thick to severely spread out the energy width of such α or ^3He peaks).

The energy of the incident beam (18.8 MeV) was determined in two ways by a kinematic null method⁸ with an estimated precision of $\pm 100\ \text{keV}$. This measurement also gave a value of $0.3 \pm 0.1^\circ$ for left-right asymmetry of the incident beam relative to the angle coordinates of the scattering chamber.

Over-all energy resolution for the experimental data ranged from 75 to 100 keV, depending on angle. Contributions to this include 15- to 50-keV target spread (depending on reaction angle), 10 keV from electronics; about 50 keV from the detector, about 50 keV from the cyclotron, and up to 20 keV-kinematic spread (due to

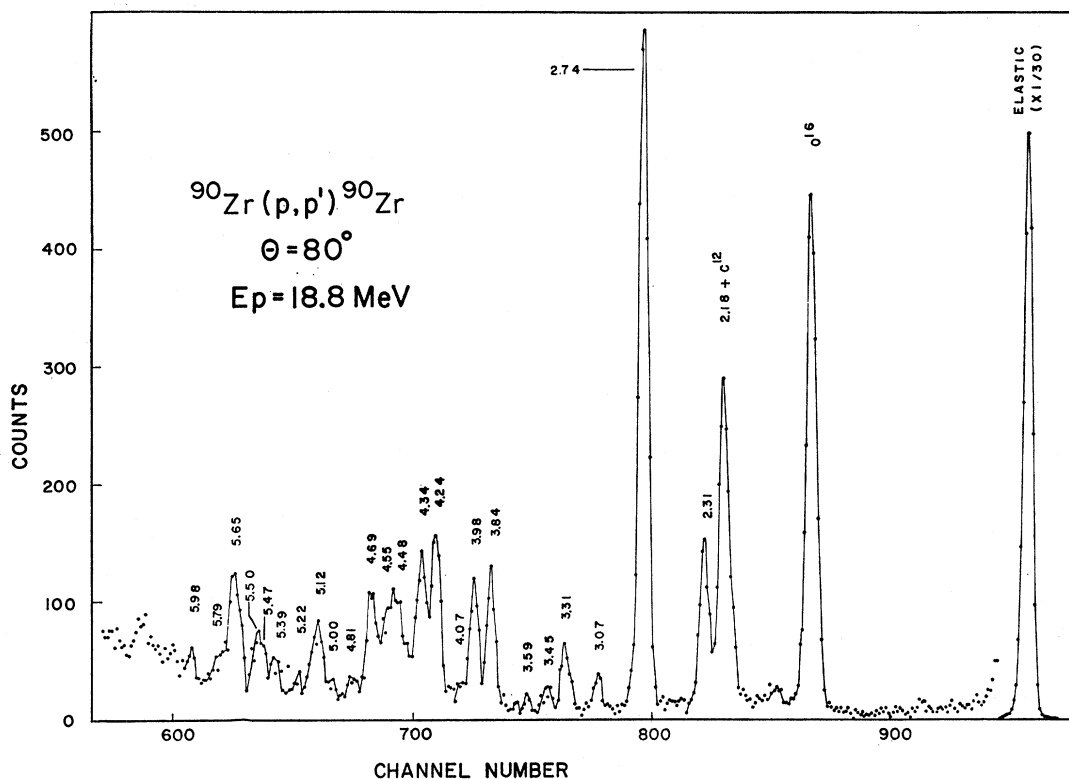


FIG. 1. A typical spectrum for 18.8-MeV protons incident on ^{90}Zr , taken at $\theta_{\text{lab}} = 80^\circ$.

⁷ P. W. Allison, Rev. Sci. Instr. 35, 1728 (1964).

⁸ B. M. Bardin and M. E. Rickey, Rev. Sci. Instr. 35, 902 (1964).

$\Delta\theta$ in the reaction plane). There was also evidence that pile-up of small pulses at extreme forward and backward angles contributed to the energy width but we make no estimate for this effect.

The data were obtained from the analyzer on punched paper tape, and fed into an automatic plotting routine.⁹ Backgrounds were estimated and peak intensities were individually summed. In cases where peaks overlap, a basic shape was taken from strong isolated peaks in the spectrum and used to extract the members, if possible. Error bars on the data are the statistical error and background uncertainty, in the case of single peaks, but include an additional error estimate if the peak was a member of a partially resolved doublet or multiplet.

Owing to the nature of the silicon solid-state detector, a small satellite peak proportional to the elastic-peak intensity appears approximately 1.85 MeV from the elastic peak. This represents the small fraction of incident charged particles leaving a ^{28}Si lattice atom in the first 2^+ excited state, effectively losing the energy of the de-excitation γ ray. This satellite falls on the 0^+ first excited state of ^{90}Zr and prevented our obtaining any information on this state except very rough upper limits for its cross section.

III. RESULTS

Data were obtained at 5° intervals from $\theta_{\text{lab}} = 15^\circ$ to $\theta_{\text{lab}} = 165^\circ$ for the proton elastic-scattering peak. Additional data points were obtained at $2\frac{1}{2}^\circ$ intervals in regions where this distribution showed minima. Useful data on most of the inelastic states extended from 20° to 100° in 5° steps and from 110° to 140° in 10° steps, although the angular distribution for the strong 2.75-MeV state was obtained out to 160° .

A typical pulse-height spectrum is shown in Fig. 1. The Q value of each state in ^{90}Zr corresponding to these peaks is shown above it. In addition, the elastic scattering peaks from various impurities are identified. States in ^{90}Zr were identified by their kinematic shift, in outgoing proton energy, as the reaction angle was changed. This eliminated the possibility of confusing excited states in light or heavy impurities with the states of interest. Although this identification procedure would not reject excited states in nuclei with $A \sim 90$ (in particular, ^{91}Zr , ^{92}Zr , ^{94}Zr , and ^{96}Zr), no evidence for the known¹⁰ excited states of these nuclei was found in the region of the pulse-height spectrum between the elastic and the first excited state of ^{90}Zr .

The energies of the outgoing protons (based on linearity of the electronics which was checked by a precision pulser unit), the incident energy, reaction angles, and mass data were used in a relativistically correct FORTRAN program⁹ to obtain Q values for each peak at

⁹ This program was written by D. Zurstadt.

¹⁰ *Nuclear Data Sheets*, compiled by K. Way *et al.* (Printing and Publishing Office, National Academy of Sciences—National Research Council, Washington 25, D. C.), NRC 60-4-26.

TABLE I. Summary of results and comparison with previous work.

Excitation energy (MeV)	This work		Previous work ^a	
	Angular distribution range	L	Excitation energy (MeV)	J^π
0	15° – 165°	0	0	0^+
1.75 ± 0.050	1.752	0^+
2.18 ± 0.015	20° – 130°	2	2.182	2^+
2.31 ± 0.015	25° – 140°	5	2.315	5^-
2.75 ± 0.015	20° – 160°	3	$2.745^{\text{b-d}}$	3^- and 4^-
3.07 ± 0.020	25° – 130°	4	3.081	4^+
3.31 ± 0.020	25° – 140°	(0,2)	3.30^e	1, 2
3.45 ± 0.025	45° – 140°	6	3.453	6^+
3.58 ± 0.045	50° – 140°	...	3.595	8^+
3.84 ± 0.020	25° – 140°	2	$3.89^{\text{b,e}}$...
3.98 ± 0.025	30° – 110°	(5)	3.98^{b}	...
4.06 ± 0.025	30° – 95°	(3)
4.23 ± 0.025	30° – 140°	(5)	4.25^{b}	...
4.34 ± 0.025	30° – 140°	(4)	$4.37^{\text{b,e}}$...
4.48 ± 0.040	30° – 140°
4.55 ± 0.030	30° – 140°
4.69 ± 0.030	25° – 140°	2
4.81 ± 0.025	40° – 140°
5.00 ± 0.035
5.11 ± 0.030	25° – 140°	(2,3,4)	$5.080(?)$...
5.22 ± 0.035
5.39 ± 0.035
5.47 ± 0.035	$5.44(?)$...
5.50 ± 0.035
5.65 ± 0.030	25° – 140°	(3)	$5.71(?)^e$...
5.79 ± 0.040
5.93 ± 0.040
5.98 ± 0.040

^a References 10 and 11 unless otherwise noted.

^b Reference 3.

^c Reference 13.

^d Reference 14.

^e Reference 12.

each angle studied, center-of-mass reaction angle and center-of-mass solid angle. A best Q value for each state was obtained by averaging the results from the various angles. Our results are summarized and compared with existing information^{3,10-14} on the states in ^{90}Zr in Table I and Fig. 2. The angular distributions and the theoretical curves leading to the listed L assignments are shown in Figs. 3 and 5–8, and are discussed in the following sections.

IV. THEORETICAL ANALYSIS

A. Optical-Model Analysis

The elastic scattering was analyzed in terms of an optical-model potential of the usual form

$$U(r) = -V(e^x + 1)^{-1} - 4iW_D(d/dx')(e^{x'} + 1)^{-1} + (\hbar/m_\pi c)^2 V_s \mathbf{L} \cdot \boldsymbol{\sigma}^{-1}(d/dr)(e^x + 1)^{-1},$$

where

$$x = (r - r_0 A^{1/3})/a, \quad x' = (r - r_0' A^{1/3})/a', \quad (1)$$

¹¹ S. Bjornholm, O. B. Nielsen, and R. K. Sheline, *Phys. Rev.* **115**, 1613 (1959).

¹² E. P. Lippincott and A. Bernstein, *Bull. Am. Phys. Soc.* **10**, 122 (1965).

¹³ D. L. Hendrie and G. W. Farwell, *Phys. Letters* **9**, 321 (1964); R. B. Day, A. G. Blair, and D. D. Armstrong, *ibid.* **9**, 327 (1964).

¹⁴ R. T. Wagner, E. R. Shunk, and R. B. Day, *Phys. Rev.* **130**, 1926 (1963).

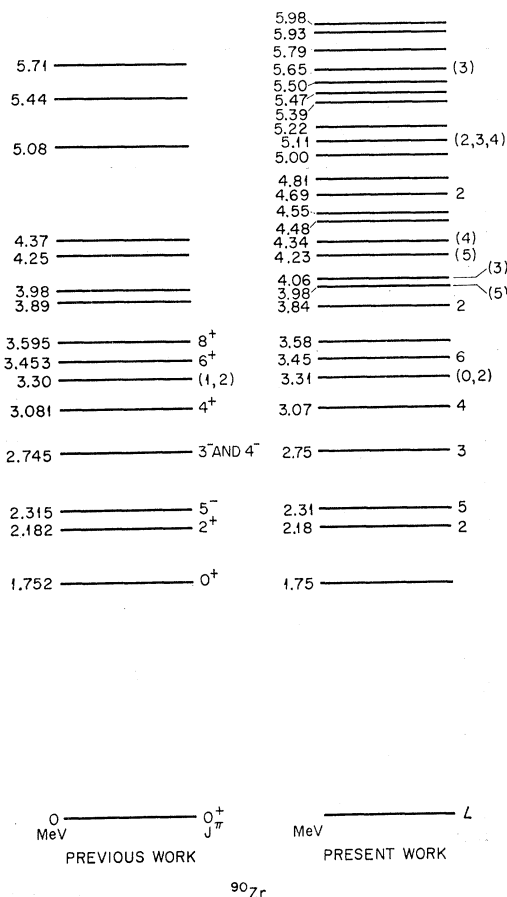


FIG. 2. Level scheme for ^{90}Zr comparing the present results with previous work. The L values shown in parentheses are tentative assignments.

to which is added the Coulomb potential for a uniformly charged sphere of radius $1.25A^{1/3}$ F. The spin-orbit strength V_s was taken to be real. The absorptive potential is of the surface type; some calculations with the addition of some volume absorption are reported below, but resulted in no improvements to the fits.

The parameter values which best fit the elastic scattering were determined by use of an automatic search routine¹⁵ which minimizes the quantity

$$\chi^2 = (1/N) \sum_{i=1}^N \{ [\sigma_{\text{TH}}(\theta_i) - \sigma_{\text{EX}}(\theta_i)] / \Delta\sigma_{\text{EX}}(\theta_i) \}^2,$$

where $\sigma_{\text{EX}}(\theta_i)$ is the measured, $\sigma_{\text{TH}}(\theta_i)$ is the calculated differential cross section at angle θ_i , and $\Delta\sigma_{\text{EX}}$ is the "error" or weight assigned to σ_{EX} . For the present purpose, χ^2 was calculated with $\Delta\sigma_{\text{EX}}/\sigma_{\text{EX}} = 10\%$ for all $N=38$ angles.

The results presented here were obtained by analysis of the cross sections alone and do not necessarily give the best fit to the polarization. Preliminary results

¹⁵ R. M. Drisko (unpublished). Some discussion of the procedure is given by E. C. Halbert, Nucl. Phys. 50, 353 (1964).

from the measurements of the polarization of 18.5-MeV protons scattered by ^{90}Zr are available,¹⁶ however, and will be discussed below. The elastic scattering has also been measured at 22.5 MeV,¹⁷ and some attempts were made to obtain optical-model potentials which were consistent with the data at both energies.

An analysis of proton scattering at energies of 9 to 22 MeV from many nuclei has been made by Perey¹⁸ and an average set of "geometrical" parameters was suggested (namely, $r_0=r_0'=1.25$ F, $a=0.65$ F, $a'=0.47$ F). The initial study of the present data was made with these parameters, and also with $V_s=7.5$ MeV, the value suggested by Perey. The best fit was obtained with $V=49.4$ MeV and $W_D=13.8$ MeV, and $\chi^2=39.9$ (Set No. 1 of Table II). As Fig. 3 shows, the predicted cross section is then too high for angles greater than about 120° . This may be improved by reducing V_s almost to zero; $V_s=1.4$ MeV (with $V=49.1$ MeV, $W_D=16.6$ MeV) gives $\chi^2=9.0$, although now the minimum at 53° is not deep enough. In addition, the predicted polarization is now much smaller than that measured (it nowhere exceeds 20%). A dramatic improvement is obtained by increasing the width a' of the absorptive potential; the optimum values are given as Set No. 2 in Table II, and have $\chi^2=3.6$. The polarization predicted is restored to reasonable values, but now the 53° minimum is displaced slightly to 56° and the 95° minimum is too deep, as Fig. 3 shows. Finally, the other three parameters were also varied, and these last two discrepancies were largely removed. The parameters for this optimum potential (Set No. 3), given in Table II, yielded $\chi^2=0.92$, and the predictions in Fig. 3. The corresponding predictions for the polarization are in quite good agreement with the preliminary measurements.¹⁶

There were indications from these calculations that the optical-model fits to the present data would be improved if the data were increased uniformly by about 10%, although this is roughly twice the estimated error

TABLE II. Optical-model parameters. (The numbers in italics were kept fixed during the search.)

	V	r_0	a	W_D	r_0'	a'	V_s	σ_R	χ^2
18.8 MeV	(MeV)	(F)	(F)	(MeV)	(F)	(F)	(MeV)	(mb)	
No. 1	49.4	<i>1.25</i>	<i>0.65</i>	13.8	<i>1.25</i>	<i>0.47</i>	7.5	1139	39.9
No. 2	47.7	<i>1.25</i>	<i>0.65</i>	9.6	<i>1.25</i>	<i>0.635</i>	5.04	1258	3.55
No. 3	55.1	1.148	0.753	7.7	1.296	0.757	6.76	1408	0.92
No. 4 ^a	54.2	1.166	0.716	8.5	1.298	0.681	6.42	1326	0.58
A ^b	52.0	1.2	0.7	9.25	1.25	0.65	6.2	1268	1.74
22.5 MeV									
5	51.6	1.186	0.778	11.1	1.268	0.587	7.36	1362	0.29
A'	50.7	1.2	0.7	9.5	1.25	0.65	6.2	1338	1.47

^a Data multiplied by 1.1 for this search.
^b Standard set, as described in text.

¹⁶ E. T. Boschitz, R. W. Bercaw, and J. S. Vincent (private communication). We are indebted to these authors for making their results available to us.

¹⁷ J. B. Ball, C. B. Fulmer, and R. H. Bassel, Phys. Rev. 135, B706 (1964).

¹⁸ F. G. Perey, Phys. Rev. 131, 745 (1963).

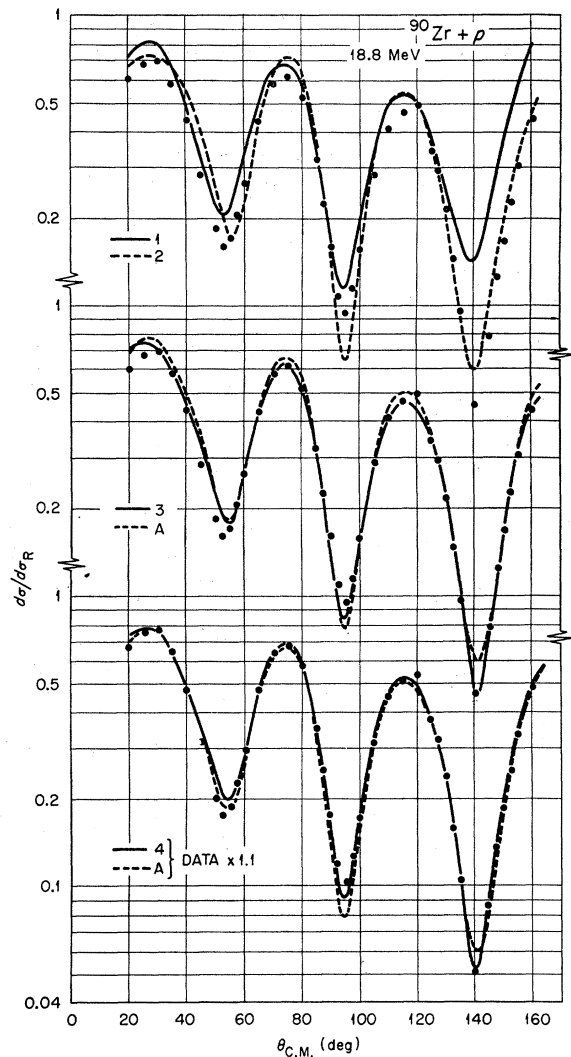


FIG. 3. Comparison of the measured elastic differential cross sections at 18.8 MeV with the predictions of the optical potentials given in Table II.

on the absolute normalization. For example, following the procedure just outlined, the χ^2 at each step was reduced to about $\frac{2}{3}$ that obtained with the original data, although the behavior of the optical-model parameters was very similar. Only about $\frac{1}{3}$ of this gain comes from the two smallest angles; the rest is distributed over the whole angular range. In illustration, the optimum set No. 4 of parameters for the renormalized data ($\chi^2=0.58$) are included in Table II, and the comparison with experiment included in Fig. 3. Although the χ^2 has been considerably reduced, subjectively the fit is little better than that to the original data. The predicted polarizations are also very similar.

Some studies were also made in which a small amount (2 MeV) of volume absorption was added to the potential (1). The effect on the optimum parameters was essentially just to reduce W_D by an equivalent amount.

However, the minimum χ^2 was increased by 50%. Hence there is no strong evidence of a need for a volume component of the absorptive potential.

Since comparable elastic data were available¹⁷ for the nearby energy of 22.5 MeV, it was of interest and value to subject this to similar analysis. The results exhibited the same features as just described for the lower energy. The optimum parameter values are included in Table II, (Set No. 5), and the predictions compared to experiment in Fig. 4. Here $\chi^2=0.29$, with $N=39$; the $\Delta\sigma_{\text{EX}}/\sigma_{\text{EX}}$ were again taken as 10% at all angles.

The "best fit" real potentials at both energies are distinguished by radius parameters of less than 1.2 F and surface diffusivities of greater than 0.7 F. Similarly, the imaginary potentials show significantly larger widths than that originally suggested for nucleons.¹⁸ This last feature produces the greatest improvement in fit, and has been previously noticed for proton scattering from some heavier elements.¹⁹ Nonetheless, the other parameter changes are believed to be significant also. Many other calculations were made with different starting values and different modes of search, but all led to the same general conclusions. Indeed, the trend for the real potential ($r_0 \sim 1.20$ or less, $a \sim 0.7$ or greater) is one previously found in an analysis of the scattering of 40-MeV protons.²⁰ At this higher energy, the surface absorption was found to be peaked *inside* the real potential ($r_0' \sim 1.1$), but it is to be expected that the form of the absorption potential will vary with energy. The behavior found in the present analysis is also similar to that found in a study²¹ of proton scattering from ^{40}Ar at energies of 8 to 14 MeV, namely $r_0 \sim 1.20$ F, $r_0' \sim 1.25$ F.

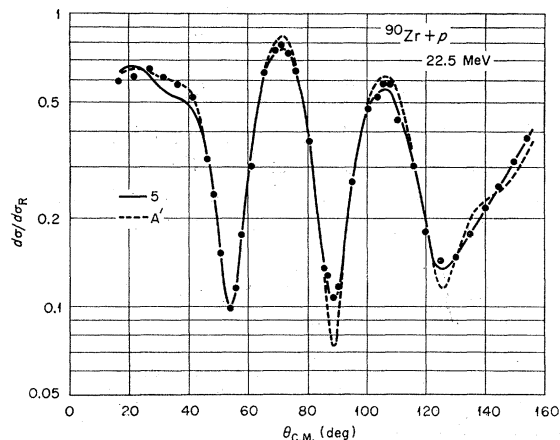


FIG. 4. Comparison of the measured elastic differential cross sections at 22.5 MeV with the predictions of the optical potentials given in Table II.

¹⁹ F. G. Perey, Argonne National Laboratory Report ANL-6848 (unpublished).

²⁰ M. P. Fricke and G. R. Satchler, Phys. Rev. **139**, B567 (1965).

²¹ G. R. Satchler (unpublished).

The optimum potential at 22.5 MeV has a smaller value of a' and a larger value of W_D than that at 18.8 MeV, but their product $a'W_D = 25.9$ MeV F is little more than at the lower energy, where $a'W_D = 23.4$ MeV F. The remaining difference is accounted for by the compensating difference in r_0' values. The differences in the real potential parameters are also well within the uncertainties of the analysis and also ambiguities of the Vr_0^n type.

For the purpose of a distorted-wave analysis of the inelastic scattering, a representative set of optical parameters was sought which would give a good account of the elastic data without necessarily being the best-fit set. The "set A" of Table II was decided upon. Comparison with the final parameter values of Table II shows that this set A is not the optimum average for the two sets of data studied here, but it was judged quite adequate in view of the small uncertainties in the parameters. The curves in Fig. 3 show that its predictions are in good agreement with experiment. When set A was used for the initial values in a search for the optimum V and W_D (the other parameters being kept fixed), the values $V = 51.9$ MeV, $W_D = 9.55$ MeV, and $\chi^2 = 1.61$ were obtained at 18.8 MeV, and $V = 50.7$ MeV, $W_D = 9.48$ MeV, and $\chi^2 = 1.47$ at 22.5 MeV. The difference in V is just that expected for an energy dependence $V = \text{constant} - \frac{1}{3}E$.

The reaction or absorption cross sections σ_R predicted by the various optical potentials are included in Table II; they are encompassed by $\sigma_R = 1274 \pm 134$ mb. The largest value is predicted by the best-fit potential, the smallest by the original parameters of Perey.¹⁸ However, the increased a' of potential No. 2 (or the set A) gives a value differing by only 10% from the optimum (No. 3) predictions; it is doubtful if measurements at the present time could distinguish between these.

B. Inelastic Scattering Theory

The inelastic scattering induced by the interaction V between the projectile proton and the target nucleus ^{90}Zr was calculated in the distorted-wave approximation.²² The transition amplitude then has the form

$$T = \int \chi_f^{(-)*}(\mathbf{k}_f, \mathbf{r}) \langle f | V | i \rangle \chi_i^{(+)}(\mathbf{k}_i, \mathbf{r}) d\mathbf{r}. \quad (2)$$

The distorted waves $\chi(\mathbf{k}, \mathbf{r})$ for momentum \mathbf{k} were generated using the optical-model potential A described in the previous section. (Calculations were also made using the best-fit potentials, but the differences were found to be negligible.) The remaining factor in the amplitude (2) is the matrix element of V between the initial and final internal nuclear wavefunctions. Most of the present discussion uses the shell model for these wave functions. However, the strongly excited 3^- state

²² See, for example, G. R. Satchler, Nucl. Phys. **55**, 1 (1964), and other references cited there.

at 2.75 MeV seen in the present experiment is probably best interpreted as a collective octupole vibration.

1. Collective Model

Most inelastic-scattering experiments have been described in terms of the collective model, which uses a nonspherical optical potential. The spherical part may then be considered to produce the elastic scattering, while the nonspherical parts are identified with the interaction V of Eq. (2) which gives rise to the inelastic scattering. The relevant theory has been described in detail elsewhere²³ and will not be repeated here except to remark that the parameters of V are then determined by the elastic scattering, except for its strength. This is expressed as a deformation parameter β_L .

Previous use of the collective model has indicated that both the real and imaginary parts of the optical potential should be deformed, so the interaction V becomes complex. The same result was found here; angular distributions in better agreement with experiment are obtained with the complex V . Figure 5 shows a comparison of theory with experiment for the 2.18-MeV $L=2$ and 2.75-MeV $L=3$ transitions. As already remarked, it is not unnatural to regard the 3^- level as an octupole vibration, and the value $\beta_3 = 0.16$ required is consistent with values for similar states in other nuclei. On the other hand, the 2^+ level is thought to be well described as a state of two protons in the $g_{9/2}$ orbit and the collective model is presumably not appropriate. This

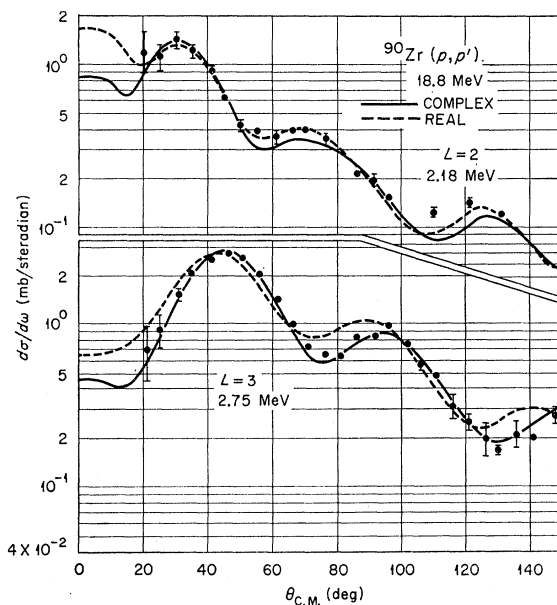


FIG. 5. Comparison of the measured differential cross sections for exciting the 2^+ and 3^- levels in ^{90}Zr with the predictions of the collective model using potential A of Table II. Coulomb excitation was included.

²³ R. H. Bassel, G. R. Satchler, R. M. Drisko, and E. Rost, Phys. Rev. **128**, 2693 (1962).

conclusion is supported by the small value of $\beta_2=0.07$ which is required, despite the good fit to the angular distribution. A typical value for a quadrupole vibrational state is $\beta_2\approx 0.2$, which represents nearly an order of magnitude larger cross section.

Two versions of the theory are shown in Fig. 5. One is that in which only the real part of the optical potential is deformed ("real"), while the other assumes both real and imaginary parts have the same deformation ("complex"). Clearly the complex coupling gives a much better fit to the measured 3^- distribution, whereas the 2^+ data are somewhat better fit with real coupling. Previous analyses of strongly excited or "collective" states have favored the use of complex coupling. It remains to be seen whether the preference for real coupling shown by the 2^+ state here is related to its lack of "collectivity." The cross-section magnitudes also depend upon the coupling assumed; the "real" curves in Fig. 5 use $\beta_2=0.09$ and $\beta_3=0.19$, both significantly larger than the values obtained with complex coupling.

Similar calculations were made for the $L=4, 6$, and 8 states at $3.07, 3.45$, and 3.59 MeV, respectively (also believed due to the $g_{9/2}^2$ configuration) and the $L=5$ state at 2.31 MeV (believed to be $g_{9/2}p_{1/2}$). The angular distributions are fit well, and the β_L values required with complex coupling are given in Table III. Although we do not regard these as vibrational states, it is of some interest to see what effective values of β_L are required for such "single-particle" transitions when the collective-model interaction is used. The predicted angular distributions are known to be relatively insensitive to the form of the interaction; they are largely determined by the L transfer and the elastic distortions.

2. Shell Model

We assume that the incident proton p interacts with each target nucleon i through a local, real, and central two-body interaction of the form¹

$$v_{ip} = -(V_0 + V_1 \sigma_i \cdot \sigma_p) g(r_{ip}), \quad (3)$$

where

$$V_S = C_{S\alpha} + V_{S\beta} \sigma_i \cdot \sigma_p. \quad (4)$$

The interaction V appearing in the amplitude (2) is then this potential summed over all the target nucleons, $V = \sum_i v_{ip}$. The various multipole terms from the expansion^{24,25} of the radial dependence $g(r_{ip})$ supply the angular momentum transfer L . The second term of (3) allows the additional transfer of $S=1$ through what we might call spin flip. The total transfer is then the vector sum of these, $\mathbf{J} = \mathbf{L} + \mathbf{S}$. The first term of (3) corresponds to $S=0$, so we only have $J=L$ for this term. The parity change is given by $(-)^L$.

²⁴ D. M. Brink and G. R. Satchler, *Angular Momentum* (Oxford University Press, New York, 1962).

²⁵ For a more detailed description see M. B. Johnson, L. W. Owen, and G. R. Satchler, following paper, *Phys. Rev.* **142**, 748 (1966).

TABLE III. Deformation parameters for the complex interaction required to fit the data shown in Figs. 5 and 6.

Energy (MeV)	2.18	2.31	2.75	3.07	3.45	3.59
L	2	5	3	4	6	8
β_L	0.07	0.075	0.16	0.04	0.09	0.035

In applying this model, we neglect exchange contributions of the knock-on type in which the projectile is captured and a target proton is emitted; these are expected to be rather small.²⁶ Then, since V is a one-body operator in the space of the target nucleons, it only connects shell-model configurations which differ in the state of at most one nucleon. If the transition involves only a single configuration in both the initial and final states the nuclear matrix element factors into a radial part and a spin-angle reduced matrix element.²⁴ For the spin-independent $S=0$ term this latter is just

$$M_L = \langle f | \sum_i i^L Y_L(\theta_i \phi_i) | i \rangle, \quad (5)$$

while for the spin-flip $S=1$ term we get

$$N_{LJ} = \langle f | \sum_i T_{L1J}(\theta_i \phi_i \sigma_i) | i \rangle. \quad (6)$$

Here T_{L1J} is a tensor of rank J constructed²⁶ from the spherical harmonic $i^L Y_L(\theta_i \phi_i)$ and the Pauli spin operator σ_i . The predicted differential cross sections then have the form²⁷

$$d\sigma/d\omega = \sum_{LS} V_S^2 \sigma_{LSJ}(\theta), \quad (7)$$

where

$$\sigma_{LSJ}(\theta) = (2J+1) [M_L^2 \delta_{S0} + N_{LJ}^2 \delta_{S1}] \sigma_L(\theta). \quad (8)$$

The "single-particle" cross section $\sigma_L(\theta)$ depends only upon the radial parts of the two single-particle orbits involved in the transition; to a good approximation they are independent of the values of S and J . The strength V_S is the operator (4) averaged over the isospin of the scattered proton and the target. For the excitation of proton states, $V_S = V_{S\alpha} + V_{S\beta}$, while for neutron excitations $V_S = V_{S\alpha} - V_{S\beta}$. Excited states which can be formed by exciting either a proton or a neutron correspond to $T=0$ ($V_S = V_{S\alpha}$) or $T=1$ ($V_S = V_{S\beta}$) excitations.

For the calculations reported here we restrict ourselves almost entirely to a single configuration for the final state $|f\rangle$. The ground state $|i\rangle$ of ^{90}Zr , however, is a mixture

$$|i\rangle = a |p_{1/2}^2\rangle + b |g_{9/2}^2\rangle, \quad (9)$$

and the matrix elements M_L and N_{LJ} will depend upon the coefficients a or b . Their values extracted from

²⁶ Some evidence for this is found in the calculation of the analogous terms for the $^{28}\text{Si}(n, p)$ reaction by A. Agodi and G. Schiffrer, *Nucl. Phys.* **50**, 337 (1964).

²⁷ The contributions from interference between $S=0$ and $S=1$ have been shown to be negligible (R. M. Haybron, private communication).

TABLE IV. The nuclear matrix elements of Eqs. (5) and (6) evaluated for the initial configuration of Eq. (9). The triads (LSJ) denote the quantum numbers; when $S=0$, the entry below is M_L , and when $S=1$, the entry below is N_{LJ} .

Final state	M_L, N_{LJ}									
$g_{9/2}^2$	(202)	(404)	(606)	(808)						
	0.278 <i>b</i>	0.200 <i>b</i>	0.154 <i>b</i>	0.113 <i>b</i>						
$p_{1/2}^{-1}g_{9/2}$	(314)	(514)	(505)	(515)						
	0.396	0.044	0.269	0.295						
$p_{1/2}^{-1}d_{5/2}$	(112)	(303)	(313)	(312)						
	-0.553 <i>a</i>	-0.370 <i>a</i>	-0.426 <i>a</i>	-0.113 <i>a</i>						
$p_{1/2}^{-1}s_{1/2}$	(101)	(111)	(110)							
	-0.326 <i>a</i>	-0.461 <i>a</i>	-0.564 <i>a</i>							
$p_{3/2}^{-1}g_{9/2}$	(303)	(313)	(314)	(505)	(515)	(516)				
	-0.390 <i>a</i>	-0.338 <i>a</i>	0.329 <i>a</i>	-0.220 <i>a</i>	-0.120 <i>a</i>	0.465 <i>a</i>				
$f_{5/2}^{-1}g_{9/2}$	(112)	(303)	(313)	(314)	(505)	(515)	(516)	(707)	(717)	
	0.603 <i>a</i>	0.144 <i>a</i>	0.332 <i>a</i>	0.288 <i>a</i>	0.211 <i>a</i>	0.308 <i>a</i>	0.179 <i>a</i>	0.342 <i>a</i>	0.365 <i>a</i>	
$p_{3/2}^{-1}p_{1/2}$	(011)	(202)	(212)	(211)						
	-0.376 <i>b</i>	-0.252 <i>b</i>	0.309 <i>b</i>	-0.133 <i>b</i>						
$f_{5/2}^{-1}p_{1/2}$	(202)	(212)	(213)	(413)						
	-0.309 <i>b</i>	-0.252 <i>b</i>	-0.057 <i>b</i>	0.395 <i>b</i>						
$g_{9/2}^{-1}d_{5/2}$	(202)	(212)	(213)	(404)	(414)	(413)	(415)	(606)	(616)	(617)
	-0.477 <i>a</i>	0.389 <i>a</i>	0.345 <i>a</i>	-0.288 <i>a</i>	0.129 <i>a</i>	-0.109 <i>a</i>	0.370 <i>a</i>	-0.197 <i>a</i>	0.061 <i>a</i>	0.500 <i>a</i>
$g_{9/2}^{-1}s_{1/2}$	(404)	(414)	(415)							
	-0.297 <i>a</i>	0.266 <i>a</i>	0.399 <i>a</i>							

experiment²⁸ range from $a^2=0.78$, $b^2=0.22$ to $a^2=b^2=0.50$. Structure calculations yield $a^2 \approx 0.64$, $b^2 \approx 0.36$ and indicate b/a is negative.²

Since the target ^{90}Zr has zero spin, J must equal the spin of the excited state. Further, the parity of the excited state is given by $(-)^L$. Then "normal parity" states, those with spin J and parity $(-)^J$, can only be excited with a transfer $L=J$, while those with non-normal parity $(-)^{J+1}$ can only be excited with spin flip $S=1$. If both the ground and excited levels are states of a j^n configuration (so L must be even), then N_{LL} vanishes and spin flip $S=1$ excitation is forbidden.²⁵ This holds for the 2^+ , 4^+ , 6^+ , and 8^+ levels of the $g_{9/2}^2$ proton configuration; the $p_{1/2}^2$ part of the ground state (9) does not contribute and only $S=0$ is allowed. The corresponding values of M_L are given in Table IV. Spin flip can contribute to the excitation of other configurations, such as the 4^- and 5^- levels of the $p_{1/2}g_{9/2}$ proton configuration. The 5^- has normal parity so $L=J=5$, but both $S=0$ and $S=1$ can contribute. Both terms of the ground state contribute, but the same single-particle matrix element is involved in both. We find from Eqs. (5) and (6),

$$\begin{aligned} M_5 &= 0.2689a - 0.1203b, \\ N_{55} &= 0.2946a + 0.1318b. \end{aligned} \quad (10)$$

If we take $a=0.8$, $b=-0.6$ then $M_5=0.287$, $N_5=0.157$. The 4^- state is particularly interesting because it is of non-normal parity and only the $S=1$ interaction contributes. We may have $L=3$ or 5 , and

$$\begin{aligned} N_{34} &= -0.2974a + 0.1330b, \\ N_{54} &= 0.0665a - 0.0297b. \end{aligned} \quad (11)$$

²⁸ R. B. Day, A. G. Blair, and D. D. Armstrong, Phys. Letters **9**, 327 (1964); N. H. Lazar, G. D. O'Kelly, J. H. Hamilton, L. M. Langer, and W. G. Smith, Phys. Rev. **110**, 513 (1958); J. L. Yntema, Phys. Letters **11**, 140 (1964).

The values $a=0.8$, $b=-0.6$ give $N_{34}=-0.318$, $N_{54}=0.071$.

The 0^+ excited state at 1.75 MeV is another special case. Its wave function is believed to be the complement of that for the ground state, Eq. (9). If it and the ground state had been pure ($a=1$, $b=0$), its excitation would have been strictly forbidden because it requires the excitation of *two* nucleons. Even with mixing the transition is considerably inhibited, the nuclear matrix element being proportional to ab times the difference between the radial form factors²⁵ for $2p_{1/2}^2$ and $1g_{9/2}^2$,

Besides the $g_{9/2}^2$ and $g_{9/2}p_{1/2}$ proton states just discussed, the lowest ^{90}Zr states (say in the first 5 MeV) may be expected from exciting a single proton from the filled $2p_{3/2}$ or $1f_{5/2}$ orbits into the $1g_{9/2}$ or $2p_{1/2}$, leaving the other two protons coupled to zero in the $p_{1/2}$ or $g_{9/2}$ orbits. This yields the proton configurations $(p_{1/2}^2)_0 p_{3/2}^{-1}g_{9/2}$, $(p_{1/2}^2)_0 f_{5/2}^{-1}g_{9/2}$, $(g_{9/2}^2)_0 p_{3/2}^{-1}p_{1/2}$ and $(g_{9/2}^2)_0 f_{5/2}^{-1}p_{1/2}$. In about the same energy range one could expect neutron excitations $g_{9/2}^{-1}d_{5/2}$ and $g_{9/2}^{-1}s_{1/2}$. Perhaps a little higher the configurations $p_{1/2}^{-1}d_{5/2}$ and $p_{1/2}^{-1}s_{1/2}$ should appear; both neutrons and protons may participate and states of " $T=0$ " and " $T=1$ " character should result. When the various total angular momenta J to which these may couple are considered, these extra configurations yield 30 states, 15 with normal parity $\pi=(-)^J$, and 15 with non-normal parity $\pi=(-)^{J+1}$. Of course, residual interactions will displace and mix these states, and states from other configurations may appear. Nonetheless, this simple zero-order picture may be used as a guide to the number and type of states to be found in the range of excitation studied in the present experiment, namely the lowest 5 or 6 MeV. Further, we might note that roughly half the states will have non-normal parity and can only be excited with spin flip. If it should appear that the spin-

flip interaction V_1 is much weaker than the spin-independent V_0 , these states are likely not to be seen.

The values of the matrix elements M_L and N_{LJ} between the ground-state (9) and the pure configurations just discussed are included²⁵ in Table IV.

Coulomb excitation may also contribute to the inelastic scattering. The nonrelativistic Coulomb interaction is a special case of Eq. (3) with $S=0$, and may easily be included. Calculations show it has negligible effect on $L>2$ transitions. When including Coulomb excitation we must be prepared to assign effective charges²⁹ e_i to the target nucleons, especially for $L=2$ quadrupole transitions. For example, measurements of the $E2$ transition rates for the 0^+ to 2^+ states of the $g_{9/2}^2$ protons in ^{92}Mo , and the 8^+ to 6^+ states of the same configuration in ^{90}Zr and ^{92}Mo , yield²⁹ $e_i\langle r^2 \rangle \approx 50 \text{ eF}^2$. The value of $\langle r^2 \rangle$ for the $g_{9/2}$ orbit used in the present calculations is 22.9 F^2 , which gives $e_i \approx 2.2e$ for the $g_{9/2}$ protons. This effective charge of about twice the charge on a free proton is assumed to come about because the proton slightly polarizes the core. However, the degree of polarization is not the same for all multipoles; usually it is greatest for quadrupoles. This concept of effective charge is not restricted to electromagnetic interactions, and we might expect to find comparable enhancement of the $L=2$ transition induced by the specifically nuclear interaction (3), compared to those for larger L . The Coulomb excitation for other $L=2$ transitions was calculated assuming that $(e_i\langle r^2 \rangle/V_0)$ had the same value as found below for the excitation of the first 2^+ state.

C. Application of Shell Model to Experimental Data

1. The $g_{9/2}^2$ and $p_{1/2}g_{9/2}$ States

Only the configuration assignments $g_{9/2}^2$ and $p_{1/2}g_{9/2}$ for the two protons are relatively unambiguous,² and attention will be concentrated on the excitation of the states of these configurations. In this way we hope to learn whether the simple model discussed in the previous section is adequate, and, if so, to learn something of the parameters of the effective interaction (3). In principle the observation of the $g_{9/2}^2$ states is particularly useful because it singles out, one by one, the even multipoles of the interaction from $L=0$ to $L=8$. The corresponding angular distributions and relative cross sections then place quite severe restrictions on the shape and range of the radial dependence $g(r)$, while the absolute cross sections determine the strength V_0 . The excitation of the 5^- state of the $p_{1/2}g_{9/2}$ configuration depends upon the $L=5$ multipole, but may be excited with $S=1$ spin flip also. However, Eq. (10) shows $N_5 \approx \frac{1}{2}M_5$ for this state, so the spin-flip cross section is only about $\frac{1}{4}$ that for $S=0$ even if $|V_1| = |V_0|$, as for a Serber force. It is very unfortunate that it has not been possible to resolve the 4^- level^{13,14} of this configuration from the close and strongly excited 3^- level at 2.75 MeV, for this would

give an unambiguous measure of the spin-flip interaction strength.

Two models were used for the radial dependence $g(r)$, a Gaussian and a Yukawa shape. The single-particle wave functions were calculated for a proton bound by 5.68 MeV ($1g_{9/2}$) or 6.6 MeV ($2p_{1/2}$) in a Woods-Saxon potential well, in the way described in the following paper.²⁵ The differential cross sections were then calculated for various ranges of the interaction, and compared to the measured cross sections. Two features emerged.²⁵ The strength of the high-multipole cross sections compared to the low multipoles is very sensitive to the range of the interaction. Secondly, the longer the range, the more structure appears in the angular distributions. This latter feature rules out a zero-range force immediately. Indeed it was not found possible to obtain reasonable agreement with both angular distributions and relative cross sections using the Gaussian shape, whereas this could be achieved with a Yukawa,

$$g(r) = e^{-\alpha r}/\alpha r,$$

with a range of about 1 F; that is, $\alpha \approx 1 \text{ F}^{-1}$. However, even then there are some reservations. Figure 6 compares the predictions with $\alpha = 1 \text{ F}^{-1}$ to the experimental cross sections. The strength used for the $g_{9/2}^2$ states was $(V_0 b)^2 = 1.52 \times 10^4 \text{ MeV}^2$ except that a value $2.15 \times 10^4 \text{ MeV}^2$ was needed for the 2^+ level. This enhancement of the quadrupole transition by 40% had been anticipated above. If $b^2 = 0.36$, this corresponds to $V_0 = 205 \text{ MeV}$ (or 244 MeV for the 2^+). The 2^+ , 4^+ , and 6^+ predictions are in good agreement with experiment, but the measured 8^+ cross section is several times larger than predicted. This discrepancy in magnitude persists whatever range or shape is used for the interaction. It is possible there could be contributions from targets other than ^{90}Zr which were not resolved in the extraction of the data for this very weak group.

The lowest curve of Fig. 6 is calculated for the 5^- level of the $g_{9/2}p_{1/2}$ configuration using the same parameters ($V_0 = 205 \text{ MeV}$ and $\alpha = 1 \text{ F}^{-1}$) and assuming $a = 0.8$, $b = -0.6$, and no spin flip, $V_1 = 0$. Including spin flip does not change the angular distribution, but will increase the cross section. Since an increase in the predicted curve of about 25% would not greatly worsen the agreement with experiment, the present results would also be compatible with $V_1 \approx V_0$. (Remember $N_{55} \approx \frac{1}{4}M_5$ for this transition.) So unfortunately we can conclude little about the magnitude of V_1 from this transition. Further, the fit to the angular distribution of this group is definitely poorer than those for the even-parity states (indeed, this group is better fitted by using the collective-model interaction!). The radial wave functions used in the present study yield $\langle 2p_{1/2} | r^5 | 1g_{9/2} \rangle = 3398 \text{ F}^5$. If the effective charge $e_i = e$, this gives for $a = 0.8$, $b = -0.6$ a half-life for the transition to the ground state of 0.67 sec, in good agreement with the measured half-life of 0.83 sec. This might be taken as

²⁹ J. Vervier, Phys. Letters 13, 47 (1964).

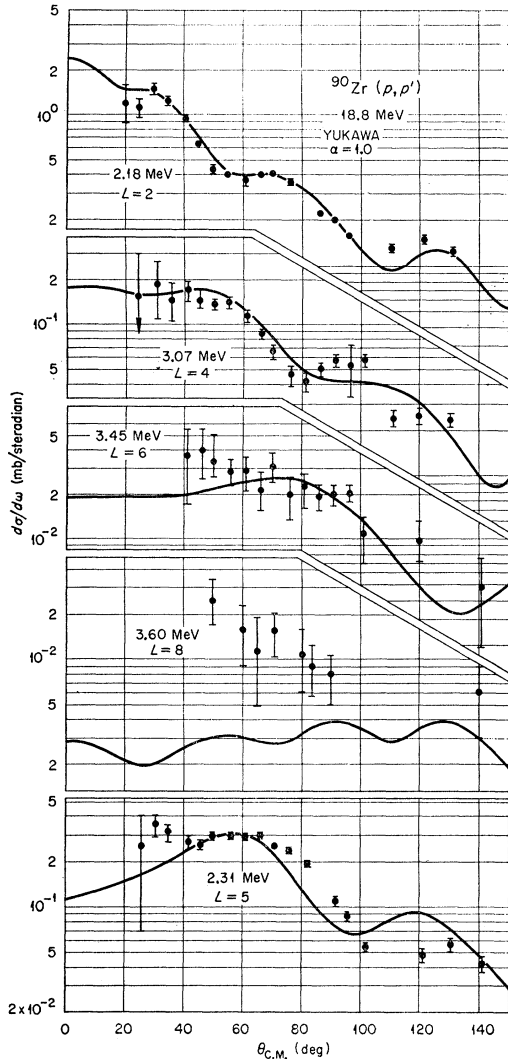


FIG. 6. Comparison of the measured differential cross sections for exciting the states of the $g_{9/2}^2$ configuration and the 5^- state of the $g_{9/2}p_{1/2}$ configuration with the predictions of the shell model. Optical potential A was used. Coulomb excitation was included for the $L=2$ transition.

evidence that the $E5$ transition is not significantly enhanced by core polarization effects.

Results for the 0^+ state at 1.75 MeV are not included in Fig. 6. Only upper limits to the cross sections at 3 angles between 40° and 60° could be determined; these are small, of the order of $20 \mu\text{b}/\text{sr}$. The predicted cross sections,²⁵ using the parameters which fit the other $g_{9/2}^2$ cross sections, are an order of magnitude *larger* than those observed. The reason for this discrepancy is not understood. It is believed it is not due to the choice of radial wave functions for the $2p_{1/2}$ and $1g_{9/2}$ orbits; reasonable changes have rather little effect on the predictions. Further, these wave functions predict

$$\langle r^2 \rangle_{g_{9/2}} - \langle r^2 \rangle_{p_{1/2}} = 2.83 F^2,$$

in good agreement with the value $2.3 \pm 0.3 F^2$ yielded by the lifetime for the monopole transition to the ground state.² The discrepancy also persists for other choices of interaction range. It may be that a more general interaction shape, such as the introduction of a repulsive core, is required, or it may be symptomatic of the inadequacy of a simple local interaction.

2. Other States

The over-all agreement between experiment and theory shown in Fig. 6 encourages us to discuss the other states in ^{90}Zr in terms of the same model. We cannot claim to deduce very much from the experimental data, but rather present this discussion as a possible interpretation of them. More work has to be done in comparing the predictions of this model to experimental results before deductions can be drawn about configuration assignments, etc., with any confidence.

As already remarked in Sec. B.2, we might expect some 30 states from the lowest excited configurations, half of which have non-normal parity and can only be excited with spin flip. In the first 5 MeV of excitation studied experimentally, only about 12 other states are seen with appreciable intensity. Calculations were made for these other configurations. The predicted differential cross sections σ_{L0L} for $S=0$ transitions to these configurations are shown in Fig. 9. They are normalized by $V_0^2 = 10^4 \text{ MeV}^2$ and assume $a^2 = 0.64$, $b^2 = 0.36$ for the ground state. The cross sections for other values of a and b , or for $S=1$, may be obtained by using Eq. (8) and Table IV. If one assumes $V_{0\alpha} = 205 \text{ MeV}$ and $V_{0\beta} = V_1 = 0$, only 11 of the normal parity states are expected to have cross sections of about $0.1 \text{ mb}/\text{sr}$ or greater at 40° . On the other hand, if $V_{1\alpha} = V_{0\alpha}$, one would expect 12 more transitions to non-normal parity states with cross sections of this order due to spin flip. The experimental results clearly imply that the spin-flip strength V_1 is appreciably weaker than the spin-independent V_0 .

A further uncertainty in the present discussion is the strength $V_{S\beta}$ of the isospin-flip interaction relative to the isospin-independent part $V_{S\alpha}$. The analysis of the $g_{9/2}^2$ excitations only yields a value for $V_0^2 = (V_{0\alpha} + V_{0\beta})^2$. If similar data for neutron scattering were available, we would have a value for $(V_{0\alpha} - V_{0\beta})^2$. Measurements on other nuclei of excitations of identical-nucleon configurations (such as the $f_{7/2}^4$ proton configuration of ^{52}Cr) have not revealed any marked differences in strength for neutron or proton scattering, which suggests that $V_{0\beta} \ll V_{0\alpha}$. In the absence of further information we shall assume $V_{0\beta} = 0$.

One level it would be particularly interesting to identify is the 1^+ state of the $(p_{3/2}^{-1}p_{1/2})$ proton configuration. Being of non-normal parity it can only be excited by spin flip; further it would be an $L=0$ transition with a forward-peaked angular distribution. A

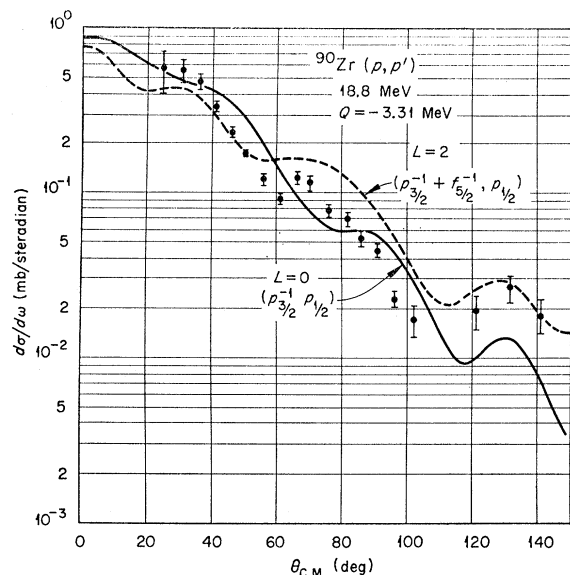


FIG. 7. The measured differential cross sections for exciting the 3.31-MeV state in ^{90}Zr . The predictions for an $L=0$ transition assume this state is 1^+ and excited by spin flip. The $L=2$ predictions assume 2^+ with an equal mixture of $p_{3/2}$ and $f_{5/2}$ excitations and includes Coulomb excitation.

possible candidate for this assignment is the 3.31-MeV level; the angular distribution for this group (Fig. 7) is rather similar to the known $L=2$ transition at 2.18 MeV, but the cross section falls more rapidly with increasing angle. Figure 7 compares the predicted $L=0$, $S=1$ angular distribution with the experimental results for this group; the interaction strength used is $(V_1b)^2 = 780 \text{ MeV}^2$, which is 20 times smaller than the spin-independent strength needed for the $g_{9/2}$ states. The experimental angular distribution is only reproduced qualitatively. Of course, it has been assumed the spin-flip interaction has the same range $\alpha = 1 \text{ F}^{-1}$ as the spin-independent part. However, although using a shorter range improves the fit somewhat, the improvement is not very great.

On the other hand, if we assign $L=2$ to this 3.31-MeV transition, the likely configurations are $(f_{5/2}^{-1}p_{1/2})$ or $(p_{3/2}^{-1}p_{1/2})$ protons, or probably a mixture of the two. The dashed curve in Fig. 7 shows the predictions for $(V_0b)^2 = 10^4 \text{ MeV}^2$ including Coulomb-excitation effects, if an equal mixture of these two configurations is assumed. [The predictions for the pure configurations are included in Fig. 9. Pure $f_{5/2}$ excitation would require $(V_0b)^2 \approx 3 \times 10^4 \text{ MeV}^2$.] Although the measured cross section still falls more rapidly than these $L=2$ predictions, the structure of the angular distribution is perhaps more satisfactorily reproduced than by the $L=0$ predictions.

Despite this ambiguity, we may conclude the following. We would expect to find such a 1^+ state somewhere in the region of excitation studied, so the lack of

observation of a group of inelastic protons with the appropriate angular distribution implies that the assignment of 1^+ to the 3.31-MeV group provides an upper limit to the strength of the spin-flip interaction. Of course, this is an $L=0$ transition. If it should appear that the monopole part of the spin-flip interaction is inhibited in the same way as the spin-independent monopole discussed above (excitation of the 0^+ level at 1.75 MeV), then we have to rely upon the number of strong transitions observed to imply that $V_1 \ll V_0$.

Even with the value $(V_1b)^2 = 780 \text{ MeV}^2$, we could expect to see two other spin-flip cross sections of approximately 0.2 mb/sr at 40° . These would arise from $L=1$ excitation of the 2^- states of the $(f_{5/2}^{-1}g_{9/2})$ and $(p_{1/2}^{-1}d_{5/2})$ configurations, with the angular distributions shown in Fig. 9. There are no obvious candidates for these transitions among the proton groups observed in the present experiment. This may mean that V_1 is actually smaller, or that these 2^- levels appear at higher excitation energies.

Let us now discuss the possible normal-parity states. With the configurations assumed we expect three other 2^+ states, excited by $L=2$ transitions. The proton groups at 3.84 and 4.69 MeV have angular distributions very similar to that for the known 2^+ , $g_{9/2}$ state at 2.18 MeV, and the $L=2$ identification is unambiguous. The magnitudes of these two cross sections are also very close. We now have two alternatives. If we assign 1^+ to the level at 3.31 MeV, then $p_{3/2}^{-1}p_{1/2}$ and $f_{5/2}^{-1}p_{1/2}$ are the likely configurations for the 3.84- and 4.69-MeV levels. The cross sections for $f_{5/2}$ excitation is about $\frac{1}{2}$ that for $p_{3/2}$ excitation (see Fig. 9); the assignment $f_{5/2}^{-1}p_{1/2}$ for either state would require $(V_0b)^2 \approx 3 \times 10^4 \text{ MeV}^2$, twice the value obtained from the $g_{9/2}$ excitations. This fact, and the near equality of the two cross sections, implies considerable mixing of the two configurations such as shown in Fig. 7. This identification would put the $g_{9/2}^{-1}d_{5/2}$ 2^+ state at a higher energy; the level seen at 5.11 MeV shows an angular distribution which could be interpreted as $L=2$, although its shape is lacking in oscillatory structure.

On the other hand, if we allow the 3.31-MeV level to be 2^+ , with a $p_{3/2}^{-1}p_{1/2}$ and $f_{5/2}^{-1}p_{1/2}$ mixture, the 3.84-MeV level would most likely have the complementary mixture. The other 2^+ at 4.69 MeV would then be mostly $g_{9/2}^{-1}d_{5/2}$ neutron excitation, but the value $(V_0a)^2 \approx 10^4 \text{ MeV}$ required is small. In view of the overall uncertainties at present, it does not seem possible to draw any more definite conclusions.

The 3^- levels are of particular interest because of the "collective" 3^- at 2.75 MeV which absorbs a considerable amount of octupole strength. The collective-model interaction was used for the theoretical curves in Fig. 5, but the two models are not mutually exclusive. For example, shell-model calculations³⁰ indicate the wave

³⁰ P. D. Kunz (private communication).

function for the 2.75-MeV level is a superposition of many particle-hole configurations. It is then possible that the correct effective interaction v_{ip} would then yield a radial dependence similar to that of the collective model²⁵; this point is being investigated. The preliminary calculations just mentioned³⁰ predict that one of the principal components of this 3^- wave function corresponds to the $(p_{1/2}^{-1}d_{5/2})$ " $T=0$ " excitation. The predicted angular distribution for this excitation is very similar to that shown in Fig. 5 for the real part of the collective interaction, while the strength required, $(V_0a)^2 \approx 6 \times 10^4$ MeV², is only a little more than twice that needed for the $g_{9/2}^2$ states. That is, the observed transition is only enhanced to about twice the strength of this single-particle transition. On the other hand, an appreciable component of this configuration in the 3^- state would allow an $l_p=2$ stripping transition in the $^{89}\text{Y}(\text{He}^3, d)^{90}\text{Zr}$ reaction. Experimentally there is observed a strong $l_p=4$ transition to the almost degenerate 4^- level, with no indications of more than about 10% $l_p=2$ contribution. This indicates that only a few percent of the 3^- wave function is $(p_{1/2}^{-1}d_{5/2})$.

Two other of the configurations considered here, namely $(p_{3/2}^{-1}g_{9/2})$ and $(f_{5/2}^{-1}g_{9/2})$ proton excitations, have 3^- states. The observed enhancement of the 2.75-MeV transition, which indicates considerable mixing, also implies that the higher 3^- states will have their transition strengths somewhat depleted. The sum of the predicted cross sections for all three configurations (with $V_0=205$ MeV, $a^2=0.64$, $b^2=0.36$) is still only about 80% of the observed 2.75-MeV cross section.

The 4.06-MeV group could be interpreted as an $L=3$ transition; if a pure $p_{3/2}^{-1}g_{9/2}$ state, the strength required is $(V_0a)^2 \approx 0.35 \times 10^4$ MeV², while $(V_0a)^2 \approx 0.8 \times 10^4$ would be required for a pure $f_{5/2}^{-1}g_{9/2}$ state. However, these and other configurations are almost certainly mixed in this state also. Identification of the other 3^- is not as easy. The measured angular distributions of the 4.81, 5.11, and 5.65-MeV groups are compatible with $L=3$ (see Figs. 8 and 9). The last group is strong; for excitation of a pure $(p_{1/2}^{-1}d_{5/2})$ state it requires $(V_0a)^2 \approx 1.2 \times 10^4$ MeV², while a $(p_{3/2}^{-1}g_{9/2})$ state would require $(V_0a)^2 \approx 1.9 \times 10^4$ MeV².

Two 4^+ states are expected from the excitation of a $g_{9/2}$ neutron to the $d_{5/2}$ or $s_{1/2}$ orbits; the predicted cross sections are very similar (see Fig. 9). The 4.34-MeV group has an angular distribution consistent with these, but requires a strength $(V_0a)^2 \approx 5 \times 10^4$ MeV² nearly twice that deduced from the $g_{9/2}^2$ states. The 5.11-MeV transition could also be interpreted as $L=4$, and requires only $(V_0a)^2 \approx 3 \times 10^4$ MeV². The angular distribution from the 5.65-MeV level is also similar, but would imply an even larger $(V_0a)^2$ of about 7×10^4 MeV².

Besides the known 5^- level at 2.31 MeV, two others should appear from the $(p_{3/2}^{-1}g_{9/2})$ and $(f_{5/2}^{-1}g_{9/2})$ proton excitations. The angular distributions for the 3.98- and 4.23-MeV levels are well reproduced by the

predictions for these configurations (see Fig. 9). The 3.98-MeV state has the smaller cross section which suggests its identification as $p_{3/2}^{-1}g_{9/2}$, although the closeness of the two levels makes some mixing likely. Assuming pure states, both transitions imply $(V_0a)^2 \approx 5 \times 10^4$ MeV², which is nearly twice the value expected.

Finally, there is a 1^- , " $T=0$ ", state from the $(p_{1/2}^{-1}s_{1/2})$ excitation with a predicted cross section of about 0.15 mb/sr at 40° . Again, it is difficult to associate this level with one of those observed in the present experiment. The 4.81- and 5.11-MeV angular distributions are not too different from the predicted curve (Fig. 9); the lower energy group gives $(V_0a)^2 \approx 1 \times 10^4$ MeV² and the higher energy group $(V_0a)^2 \approx 3.3 \times 10^4$ MeV².

V. SUMMARY AND DISCUSSION

A good account can be given of the excitation of the states arising from the $g_{9/2}^2$ and $g_{9/2}p_{1/2}$ proton configurations by assuming a Yukawa interaction of range 1 F and strength 205 MeV between the incident proton and the target protons. The quadrupole transition strength to the 2^+ level is enhanced by about 40% compared to the other states.

The 12 other states observed which do not come from these configurations have been discussed in a tentative manner. The *number* of states observed is consistent with a spin-flip interaction considerably weaker than the spin-independent one. Two $L=2$ transitions with energies of 3.84 and 4.69 MeV can be positively identified, but a more complete description of the 2^+ states depends upon a choice of 1^+ or 2^+ for the 3.31-MeV level. The 4.07-MeV state is tentatively assigned 3^- , and another 3^- is expected at a higher energy, perhaps at 5.65 MeV. Two 5^- states are expected, and are likely to be those seen at 3.98 and 4.24 MeV. Unique identification of other levels is difficult, and deductions concerning their shell-model configurations are very uncertain. Nonetheless, there is nothing in the present data which is incompatible with the expectations of the shell model and the simple interaction adopted here with the parameters deduced from the $g_{9/2}^2$ states.

The effective nucleon-nucleon interaction v_{ip} deduced from the present experiment is of somewhat shorter range and considerably stronger than that required to explain the scattering of two free nucleons at low energy. In addition the spin dependence appears to be quite different. For example a Serber mixture leads to $V_0 = -V_1$, while the inelastic scattering implies $V_1 \ll V_0$. It is interesting to ask what optical potential this effective interaction would predict if we assume it is obtained by simply averaging the interaction over the nuclear matter distribution. The strength at the center of the nucleus is then approximately $4\pi V_0 \rho_0 / \alpha^3$, where ρ_0 is the nucleon density. Since $\rho_0 \approx \frac{1}{6} \text{F}^{-3}$, our present

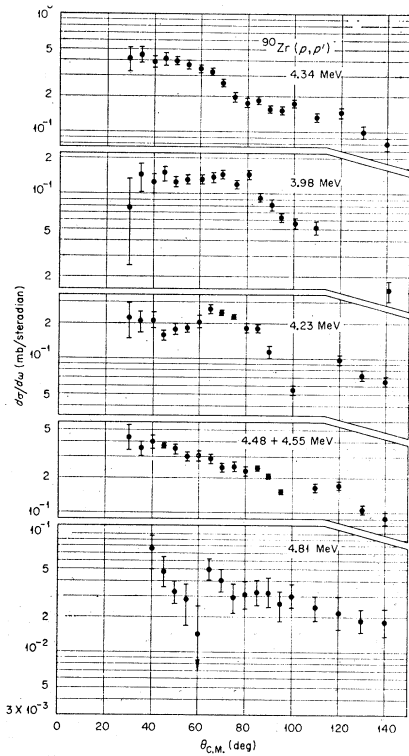
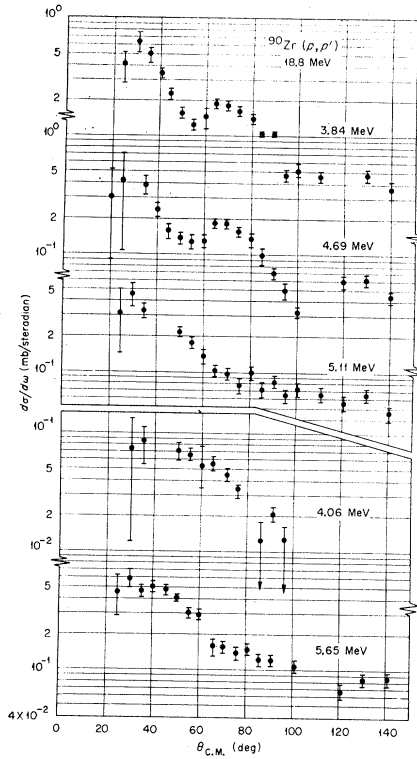


FIG. 8. Measured differential cross sections for the remaining proton groups detected in the present experiment.

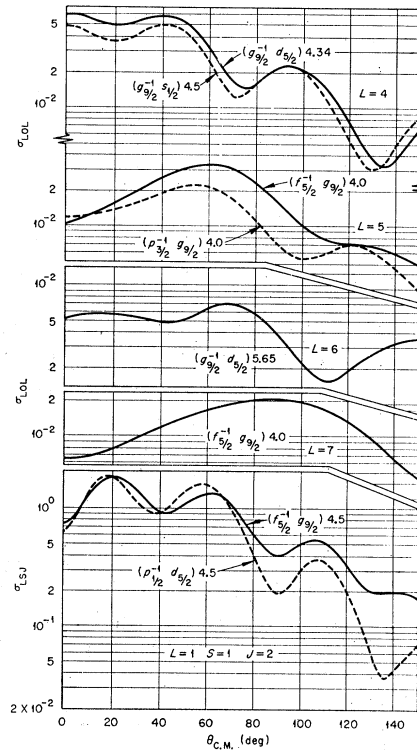
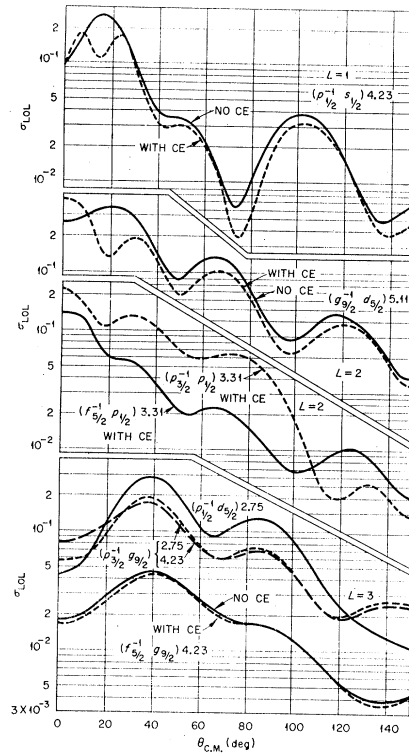


FIG. 9. Predicted differential cross sections for some other configurations expected in the lower part of the ^{90}Zr spectrum. The values $a^2=0.64$ and $b^2=0.36$ were assumed for the ground state, and $V_S=100$ MeV was used. The cross sections are proportional to V_S^2 . The dashed curve for $L=1$ includes Coulomb excitation calculated with $e_i=e$. The number appearing after each configuration is the excitation energy assumed in the calculation. As is shown for one of the $L=3$ transitions, the results are relatively insensitive to this energy.

interaction gives about 400 MeV for the optical-potential well depth, or about 8 times the empirical value. However, it might be noted that only the monopole part of the interaction contributes, and we have already seen that this predicts an excitation cross section for the 0^+ level at 1.75 MeV which is an order of magnitude larger than that observed. It remains to be seen whether these gross discrepancies are due to the inadequacy of the model potential for the monopole part of the interaction, to the neglect of exchange effects, or to some other cause.

Some of these questions may be answered by a similar analysis of proton scattering data from other nuclei

whose wave functions are probably well described by the shell model, such as those of the $1f_{7/2}$ shell.³¹

ACKNOWLEDGMENTS

We wish to express our appreciation to Margaret Stautberg, D. Zurstadt, and D. Petersen for assistance in data taking and data analysis, and to the staffs of the University of Colorado Nuclear Physics Laboratory and the University of Colorado Computing Center. We are indebted to R. M. Drisko for making available the optical-model code HUNTER and the distorted-wave code JULIE.

³¹ W. S. Gray, R. A. Kenefick, and J. J. Kraushaar, Nucl. Phys. **67**, 542 (1965); *ibid.* **67**, 565 (1965).

Shell-Model Form Factors for the $^{90}\text{Zr}(p,p')$ Reaction*

M. B. JOHNSON,† L. W. OWEN,‡ AND G. R. SATCHLER

Oak Ridge National Laboratory, Oak Ridge, Tennessee

(Received 29 September 1965)

The application of the shell model to the $^{90}\text{Zr}(p,p')$ reaction is described. The nuclear matrix elements, and particularly the radial form factors, are discussed. Interactions of Gaussian and Yukawa form between projectile and target nucleons are used. They are assumed to be central, but spin and isospin dependence is included. The shell-model orbitals are calculated for a potential of the Woods-Saxon shape. The effects of parameter variations and of corrections such as may be due to nonlocality of the potentials are studied in some detail. It is shown how the data for the $^{90}\text{Zr}(p,p')$ reaction favor a Yukawa interaction with a range of about 1 F.

I. INTRODUCTION

THE preceding paper¹ described the results of measurements on the $^{90}\text{Zr}(p,p')$ reaction at 18.8 MeV, and compared them with theoretical predictions based on the nuclear-shell model. In the present paper we examine in more detail some aspects of this model, in particular the radial form factors which arise from the nuclear matrix elements. Various features, such as the effects of including nonlocality corrections, are explored so that a better assessment can be made of the fits to experimental data and the significance of the parameters so obtained.

In order to apply the shell model, we need to assume an interaction v_{ip} between the projectile p and each target nucleon i . At high energies (say, 100 MeV or greater) it is reasonable to invoke the impulse approximation,² in which v_{ip} is replaced by the scattering am-

plitude t_{ip} for two free nucleons. However, at the lower energies with which we are concerned here, the corrections to this simple prescription are likely to be so large it is more profitable, at least initially, to regard v_{ip} as an effective interaction for which we may try various phenomenological models. The parameters of the model interaction are then to be determined by fitting to experimental data. Before this can be done we must have some knowledge of the wave functions for the target nucleus which is to be excited.

^{90}Zr is quite appropriate for this purpose since it possesses a set of excited states which appear to be due to relatively pure $(g_{9/2})^2$ and $(g_{9/2}p_{1/2})$ configurations for the last two protons.³ The first of these configurations has states of spin 0^+ , 2^+ , 4^+ , 6^+ , and 8^+ whose excitation selects out the corresponding multipoles of the effective interaction and provides a detailed probe of its structure.

The information contained in the experimental data is of two kinds. On the one hand we have the cross-section magnitudes, and in particular the relative mag-

(N. Y.) **8**, 551 (1959); R. M. Haybron and H. McManus, Phys. Rev. **136**, B1730 (1964).

³ B. F. Bayman, A. S. Reiner, and R. K. Sheline, Phys. Rev. **115**, 1627 (1959); I. Talmi and I. Unna, Nucl. Phys. **19**, 225 (1960).

* Research sponsored by the U. S. Atomic Energy Commission under contract with Union Carbide Corporation.

† Participant in Student Cooperative Program from Virginia Polytechnic Institute, Blacksburg, Virginia.

‡ Permanent address: Physics Department, University of Tennessee, Knoxville, Tennessee.

¹ W. S. Gray, R. A. Kenefick, J. J. Kraushaar, and G. R. Satchler, preceding paper, Phys. Rev. **142**, 735 (1966).

² A. K. Kerman, H. McManus, and R. M. Thaler, Ann. Phys.